ON THE MODULI SPACES OF EMBEDDED CONSTANT MEAN CURVATURE SURFACES WITH THREE OR FOUR ENDS

KARSTEN GROSSE-BRAUCKMANN AND ROBERT B. KUSNER

We are interested in explicitly parametrizing the moduli spaces $\mathcal{M}_{g,k}$ of embedded surfaces in $\mathbb{R}^3$ with finite genus g and a finite number of ends k having constant mean curvature. By rescaling we may assume this constant is 1, the mean curvature of the unit sphere. Two surfaces in $\mathbb{R}^3$ are indentified as points in $\mathcal{M}_{g,k}$ if there is isometry of $\mathbb{R}^3$ carrying one surface to the other. Moreover, we shall include in $\mathcal{M}_{g,k}$ a somewhat larger class of constant mean curvature (CMC) surfaces, the *Alexandrov embedded* surfaces, which are immersed surfaces bounding immersions of handlebodies into $\mathbb{R}^3$. The structure of these moduli spaces is known: they are finite dimensional real analytic varieties [KMP], but only a few of them are understood completely: the only embedded compact CMC surface is a round sphere [A], so $\mathcal{M}_{g,0}$ is either a point ($g = 0$) or empty ($g > 0$); $\mathcal{M}_{g,1}$ is empty, since there are no 1-ended examples [M]; and 2-ended examples are necessarily the Delaunay unduloids [KKS], which are simply-periodic surfaces of revolution whose minimal radius or *necksize* $\rho \in (0, \frac{1}{2}]$ parametrizes $\mathcal{M}_{0,2}$, whereas $\mathcal{M}_{g,2}$ is empty for $g > 0$. The Kapouleas construction [Kp] shows that $\mathcal{M}_{g,k}$ is not empty for every $k \geq 3$ and every g.

We focus on CMC surfaces with special symmetries: the submoduli space of these can be thought of as the fixed point sets of automorphisms of the (pre)moduli spaces $\mathcal{N}_{g,k}$ of CMC surfaces *before* modding out by $\mathrm{Isom}(\mathbb{R}^3)$. Each embedded end of a CMC surface is asymptotically a Delaunay unduloid [KKS], so we use the necksizes and axes of these asymptotic unduloids to describe a surface and its symmetries. In previous work [G] we considered a subset of the *k-unduloids* $\mathcal{M}_{0,k}$. We proved existence of an entire connected component of the submoduli space with dihedral symmetry: for k asymptotic axes arranged in a plane with equal angles $2\pi/k$, two k-unduloids exist for (asymptotic) necksizes in the interval $(0, \frac{1}{k})$ and one surface corresponds to the right endpoint. Note that the submoduli space of dihedrally symmetric k-unduloids is one-dimensional.

Date: Preliminary, April 22, 1996.

Supported by SFB 256 at Universität Bonn, and NSF grant DMS 94-04278 at UMassAmherst.

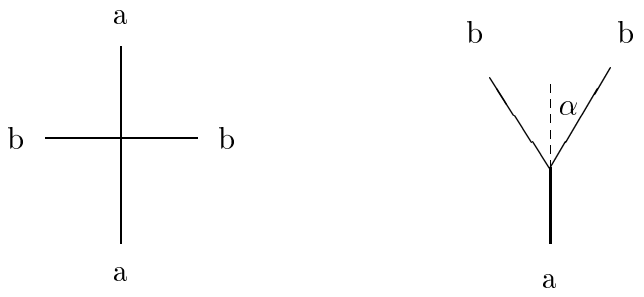

FIGURE 1. Axes of rectangular and isosceles surfaces

In the present paper some 2-dimensional submoduli spaces are studied for the first time. The triunduloids $\mathcal{M}_{g,3}$ are special in that *a priori* they always have a plane of reflection [KKS], which we will think of as a *horizontal* plane. Their moduli space is 3-dimensional at non-degenerate points [KMP]. Here we study *isosceles* triunduloids which have the additional symmetry in the form of a *vertical* plane of reflection, as depicted in Figure 1. We also study a submoduli space of the 6-dimensional space of 4-unduloids, namely the *rectangular* 4-unduloids with the two extra vertical symmetry planes depicted in Figure 1. There is no period problem in the rectangular case; it is remarkable that the balancing property and the fact that each end is asymptotically Delaunay are sufficient to solve the period problem arising for the isosceles surfaces. Furthermore, we make some remarks on the case of *rhombic* 4-unduloids and dihedrally symmetric k-unduloids of genus 1. However, the present analysis leads only to a qualitative understanding of the period problems arising for the latter two types of surfaces, and we need the quantitative information which we obtained numerically (see [GP]). These two pieces of information still lead to a complete understanding of the moduli spaces for these surfaces, which are two- and one-dimensional, respectively.

We derive necessary conditions on the class of surfaces we consider. By Lawson's theorem [Ka] [L], these follow from an analysis of the fundamental domains and their associated boundary curves. Namely, if there is a CMC surface with the assumed symmetries, then there is an associated minimal surface in the three-sphere $\mathbb{S}^3$, and its boundary consists of geodesic arcs. Moreover, adjacent spherical arcs make angles with each other which can be determined from the symmetry properties of the CMC surface. Spherical boundary polygons of these specific angular types exist only with certain lengths, and this restricts the range of necksizes of the Delaunay ends which occur. We need the symmetry assumption to guarantee that a fundamental domain is simply connected so that Lawson's theorem is applicable, and to have the number of boundary arcs low enough to handle the spherical trigonometry explicitly.

We conjecture, but do not prove, the following: (*i*) our continuous families of contours bound a continuous family of minimal surfaces in the sphere which in turn give rise to a continuous family of CMC surfaces; (*ii*) these are unique with the assumed symmetry and Alexandrov embeddedness properties. (*iii*) There are no further connected components for our symmetry types.

For the dihedrally symmetric k-unduloids we found in [G] that the necksizes $\rho_1 = \ldots = \rho_k$ of the maximal continuous family have necksize-sum

$$\sum_{j=1}^{k} \rho_j \leq 1\,. \tag{1}$$

We also proved existence, so that problem (*i*) is settled, and in the present paper we prove (*ii*) and (*iii*) for this case. For the maximal continuous families of rectangular surfaces our result is that the maximal family of associated boundary contours also has necksize-sum at most 1. However, for the isosceles surfaces, our bound on the necksize-sum depends on the angle α. The bound is 1 for angles greater than about 48 degrees, but tends to 0 when the angle tends to 0, see (28). The transition from constant to non-constant necksize-sum occurs at a surface which, surprisingly, has one cylindrical end. Although 1 might appear as a general bound on the necksize sum in $\mathcal{M}_{g,k}$ after these results, our paper also indicates (but does not prove) that rhombic 4-unduloids and k-unduloids of genus 1 exceed this necksize-sum; in the rhombic case the four ends can be as close to cylindrical as we like so that the strict upper bound on the necksize-sum is 2, see [GP].

We should mention that our approach here to studying these moduli spaces might be viewed as an example of the "mapping in" method — we seek curves or higher-dimensional parameter spaces that admit smooth maps into $\mathcal{M}_{g,k}$. Another approach is the "mapping out" method, which considers smooth maps from $\mathcal{M}_{g,k}$ to natural geometric objects, such as the *weighted axes* map to space of *balanced diagrams*, as has been explored in a very preliminary way in [K1] and more thoroughly in [K2].

1. Preliminaries

1.1. **Lawson's theorem.**

Theorem 1. [L, p.364] (*i*) *Let M be a simply connected minimal surface in $\mathbb{S}^3$. Then there exists an isometric* CMC *surface $\tilde{M} \subset \mathbb{R}^3$, and vice versa.*
(*ii*) *Furthermore, if M is bounded by a (generalized) polygon Γ of great circle arcs in $\mathbb{S}^3$ then $\tilde{M}$ is bounded by geodesic curvature lines.*

Our polygons are parameterized objects, i.e. they do not have to be embedded, and we distinguish a polygon with an arc of length l from the similar polygon where the respective arc has length $l + 2\pi$. We say *generalized polygons* since we allow for degenerate arcs having infinite length. We call such arcs *ray* or *line* if they extend in only one, or two directions to infinity.

Geodesic curvature lines are planar and arise as the boundaries of fundamental domains of CMC surfaces with respect to a group of planar reflections. On the other hand, simply connected CMC domains bounded by these lines admit smooth (Schwarz) reflection in the planes.

In the following we use the term *patch* to stand for either a simply connected CMC surface bounded by geodesic curvature lines, or a simply connected spherical minimal surface bounded by great circle arcs. Our patches are not compact. Specifically we will deal with CMC patches containing *quarter ends*, that is the portion of an end cut out by two orthogonal symmetry planes whose intersection is the axis of the end. Likewise a *half end* is to one side of one symmetry plane containing the axis.

Lemma 2. *Let $\tilde{M}$ be a* CMC *patch which contains a quarter end of necksize ρ, bounded by two geodesic curvature rays $\tilde{\gamma}, \tilde{\eta}$. The associated spherical patch is then bounded by two great circle rays γ, η. These two rays project to great circles with perpendicular great circle arcs of lengths $\pi\rho/2$ and $\pi(1-\rho)/2$, whose distance to the* CMC *patch tends to 0 when the end becomes asymptotically Delaunay. If $\rho \neq 1/4$ the perpendiculars are unique up to the antipodal map of $\mathbb{S}^3$, for $\rho = 1/4$ they form a continuous family by running through each point of the boundary rays.*

Proof. By Lawson's theorem the associated spherical patch M has geodesic boundary. Thus γ and η are geodesic rays. Each embedded end is asymptotic in distance to a Delaunay unduloid [KKS]. Thus also the associated spherical patch is asymptotic in distance to an associated Delaunay unduloid.

An unduloid has symmetry lines perpendicular meeting its meridians in right angles, namely the curvature lines of minimal and maximal radius. These lines have length $2\pi\rho$ and $2\pi(1-\rho)$, or $\pi\rho/2$ and $\pi(1-\rho)/2$ for a quarter end. Thus the isometric associated quarter unduloids contain great circle arcs of the same length perpendicular to the bounding circles. In fact the associated unduloids are the ruled surfaces obtained by joining points on these pairs of perpendiculars, where the perpendiculars are parametrized with constant speed, see [G] for an explicit parameterization. On a non-cylindrical unduloid the symmetry lines meet the meridians in distance $\pi/2$. Since short and long perpendiculars alternate (as

necks and bubbles do), this gives uniqueness up to the antipodal map. Likewise, on a cylinder each circle perpendicular to a meridian is a symmetry line, which gives the continuous family of perpendiculars having the same length $\pi/4$. □

We will need a similar statement for half ends. Unfortunately the geodesic rays do not uniquely define perpendiculars of lengths $\pi\rho$ and $\pi(1-\rho)$. Instead there is a full circle of those. In the next subsection we introduce a tool to select the pair of perpendiculars to which an associated end is asymptotic.

We need to define continuity of CMC surfaces and also of assciated boundary polygons. For the moduli of the CMC surfaces we can take the C^1-topology which is equivalent to all other C^k-topologies, $k > 1$. For the great circle polygons with fixed Hopf fields we can simply take the set of (positive) arclengths as coordinates.

Theorem 3. *Let $\mathcal{M}$ be a connected set of* CMC *surfaces, invariant under a group of reflectional symmetries G, such that the fundamental patches are simply connected. Then the the number of boundary arcs of the patch is constant, and the associated spherical minimal patches are bounded by a connected set of spherical geodesic polygons.*

Proof. The map associating the set of arclengths of the associated contour to a CMC surface is continuous. We want to show that an arclength cannot degenerate to 0. We can distinguish two cases for an arc with length tending to 0: (i) It has (in the limit) no rotation of the tangent plane, or (ii) it has a non-zero rotation. In case (ii) the tangent plane rotates, and the limit must have infinite curvature. Hence, when the edgelength tends to zero, the CMC patches do not converge in C^1. On the other hand, in case (i) the rotation of the tangent plane of the CMC surface along the short arc is either 0 or arbitrarily small. In either case there is no bound on the order of the group of reflectional symmetries, independent of the arclength. Thus the resulting surface is either simply periodic or the surface has continuous symmetries, i.e. it must be Delaunay. □

1.2. **Karcher's Hopf fields.** The spherical boundary contours associated to a given curvature line: have a property invariant of length of the polygon arcs: each arc is tangent to some fixed Hopf field. A *Hopf field* is a unit vector field tangent to the sphere $\mathbb{S}^3$, and specifically each geodesic boundary arc is contained in a great circle, being a fibre of one fixed Hopf fibration. There is an $\mathbb{S}^2$ worth of such fibrations, being defined for instance by the tangent directions at one fixed point of $\mathbb{S}^3$. For the following we use a fixed positively oriented orthonormal basis A, B, C. Thus any linear combiniation $aA+bB+cC$ with $a^2+b^2+c^2=1$ stands for a Hopf field (or a Hopf fibration) and is the invariant associated to each boundary

arc of a contour. The fields for an entire contour are only well-defined up to a rotation $\varphi \in SO_4$, and we will always make a special choice.

The fields can be read off the boundary of the CMC patch as follows: (i) subsequent fields make an angle equal to the angle of the geodesic curvature lines in a vertex (which is also the dihedral angle of the two symmetry planes containing these arcs), and (ii) the fields rotate from one vertex to the next as much as the normal rotates between to vertices on the CMC patch, the latter angle is defined in the plane containing the boundary arc.

Hopf fields were added to Lawson's conjugate surface construction by Karcher, see [Ka] or [G] for a detailed description.

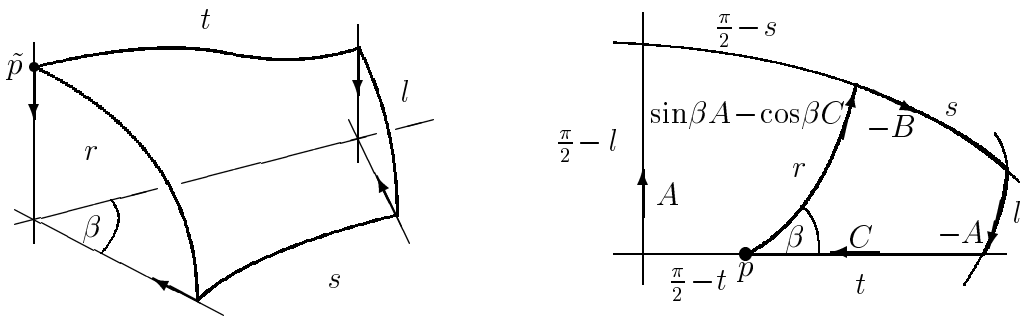

FIGURE 2. Quadrilateral bounding a Euclidean CMC and an isometric spherical minimal patch (righthand sketch is meant as a stereographic projection).

1.3. **Trigonometry.** Our analysis relies on spherical trigonometry, namely the trigonometry of the boundary polygons of the spherical minimal patches associated to the fundamental domains for the CMC surfaces with few ends. It is sufficient for our purposes to consider quadrilaterals of the type depicted in Figure 2. These quadrilaterals are characterized as follows: they have three right angles, one angle $0 < \beta < \pi$; the Hopf fields along one arc (the l-arc in Fig. 2) turn with $-\pi/2$, as they do on a capped quarter Delaunay unduloid, on the adjacent two arcs they don't turn. We denote a quadrilateral with lengths as in Figure 2 as $\Gamma(l, r, r, s; \beta)$. Its Hopf fields depend on β, and are, e.g., $-A$, C, $\sin\beta\, A - \cos\beta\, C$, $-B$ in the same order.

The two quadrilaterals $\Gamma(\pi/6, \pi/4, \pi/4, \pi/6; \pi/3)$ and $\Gamma(\pi/8, \pi/4, \pi/4, \pi/8; \pi/4)$ give rise to doubly periodic CMC surfaces studied by Lawson [L]. Let us call all quadrilaterals with the described Hopf fields and with $0 < l \leq \pi/4$ *Lawson quadrilaterals*.

We need a slightly generalized version of Lemma 3.1 in [G].

Lemma 4. *For given $0 < \beta < \pi$ there exists a continuous 1-parameter family of quadrilaterals $\Gamma(l,t,r,s;\beta)$ as follows:*
(i) If $0 < \beta < \pi/2$ the lengths l,t,r,s range from $0,0,0,0$ over $\beta/2, \pi/4, \pi/4, \beta/2$ to $0, \pi/2, \pi/2, \beta$. Here r, s, t are monotonic, whereas l monotonically increases on the first part of the family and monotonically decreases on the second half.
(ii) If $\pi/2 < \beta < \pi$ the lengths l,t,r,s range from $0,\pi,0,\pi$ over $\beta/2, 3\pi/4, \pi/4, \pi-\beta/2$, to $0, \pi/2, \pi/2, \pi-\beta$. Again r, s, t are monotonic, whereas l monotonically increases on the first part of the family and monotonically decreases on the second half.
(iii) For $\beta = \pi/2$ and $0 < r < \pi/2$ quadrilaterals exist with constant lengths $s = t = \pi/2$, and $l = \pi/2 - r$.
(iv) There are further quadrilaterals with $\beta = \pi/2$ and constant lengths $s = t = \pi$ with $0 < l = r < \pi/2$.

Proof. Part (i) was proved in [G]. We repeat the main steps of the proof and use them for the proof of (ii). We assume $0 < l,t,r,s < \pi/2$. The quadrilateral is uniquely characterized by the four formulas

$$\cos s \cos r = \cos l \cos t, \tag{2}$$

$$\sin s \cos r = \sin l \sin t, \tag{3}$$

$$\cos s \cos l = \cos r \cos t + \cos\beta \sin r \sin t, \tag{4}$$

$$\sin s \sin l = \cos r \sin t - \cos\beta \sin r \cos t. \tag{5}$$

These formulas can be obtained using the spherical cosine law. Dividing (3) by (2) gives

$$\tan s = \tan l \tan t. \tag{6}$$

Elementary calculations lead to

$$\tan 2t = \cos\beta \tan 2r, \tag{7}$$

which holds unless $r = \pi/4 \Leftrightarrow t = \pi/4$. Finally

$$\cos 2l = \cos\beta \sin 2r \sqrt{1 + \frac{1}{\cos^2\beta \tan^2 2r}} = \sqrt{\cos^2\beta \sin^2 2r + \cos^2 2r}. \tag{8}$$

A particular consequence of (8) is $\cos 2l \geq \cos\beta$.

Existence and uniqueness is obtained as follows: For each $0 \leq r \leq \pi/2$ we get a length $0 \leq l \leq \beta/2$ by (8), $0 \leq t \leq \pi/2$ by (7) and $0 \leq s \leq \pi/2$ by (6), and obtain a quadrilateral for which (2) – (5) hold. Therefore it has the desired Hopf fields.

The proof of (ii) is exactly the same. It can be seen that l, t, r, s, β solve (2) to (5) if and only if $l, \pi - t, r, \pi - s, \pi - \beta$ solve them. In particular (6) to (8) hold. Geometrically these quadrilaterals can be obtained from those of (i) as follows. We extend the s- and t-arcs in Figure 2 to the left by $\pi/2$ each, and join the endpoints with a perpendicular of length l; then the second quadrilateral is obtained to the left of the first. □

Since (6) – (8) characterize the quadrilaterals with Lawson's Hopf fields, we obtain a uniqueness for the Lawson quadrilaterals: and lengths modulo π. More precisely we have.

Lemma 5. *All Lawson quadrilaterals are generated from those listed in Lemma 4 by the following substitutions:*
(i) *Adding* $2\pi n$ *for* $n \in \mathbb{N}$ *to* r, s *or* t,
(ii) *replacing* s, t *by* $s + \pi, t + \pi$,
(iii) *replacing* r, t *by* $r + \pi, t + \pi$,
(iv) *replacing* r, s *by* $r + \pi, s + \pi$.

For the isosceles surfaces we need another type of quadrilateral which we call *Clifford rectangle*: it has four right angles and opposite lengths are equal. If the lengths are $l, r > 0$ we denote it with $\Gamma(l, r)$. These rectangles can be obtained as subsets of a Clifford torus, and the opposite arcs are Clifford parallels. We will use the fact that one pair of opposite arcs has equal Hopf fields.

1.4. **Balancing and Kapouleas' existence result.** Delaunay determined the 2-ended surfaces in the last century, but existence of surfaces with 3 or more ends was only proved recently by Kapouleas. To state the existence result for genus 0 we associate a *force*

$$f := 2\pi\rho(1 - \rho)\mathbf{a} \in \mathbb{R}^3 \tag{9}$$

to a Delaunay unduloid with necksize ρ, whose axis points in the direction of the unit vector $\mathbf{a}$. Kapouleas proved existence of surfaces with genus $g \in \mathbb{N}_0$ and $k \geq 3$ ends, asymptotic to Delaunay unduloids with force vectors arbitrarily close to $f_1, \ldots, f_k$, if the forces satisfy two conditions: they are balanced,

$$\sum_{k=1}^{n} f_k = 0, \tag{10}$$

and small, i.e. $|f_1|, \ldots, |f_n| < \epsilon$ holds for some $\epsilon > 0$. The necessity of the condition (10) was proved by one of the authors [K1] in much greater generality using an integral representation of the force. Kapouleas' condition on the forces means

that the necksizes are small; we will see below that very interesting phenomena occur for large necksizes.

2. Dihedrally symmetric k-unduloids

We discussed these surfaces already in [G]. However, there the emphasis was on existence, whereas here we would like to provide what is needed to show uniqueness. In the next Lemma we relate fundamental domains of the dihedrally symmetric k-unduloids to the Lawson quadrilaterals with angle $\beta = \pi/k$.

Lemma 6. *A fundamental domain of a dihedrally symmetric k-unduloid is associated to a spherical minimal patch bounded by degenerate triangle T with two great circle rays and one great circle arc of length $0 < r < \pi/2$. Truncation of the degenerate triangle leads to a Lawson quadrilateral $\Gamma(l, t, r, s; \pi/k)$ with $0 < l \leq \pi/4$.*

Proof. By the Alexandrov reflection principle in the form described in [KKS] a dihedrally symmetric k-unduloid is symmetric with respect to the horizontal symmetry plane containing the axes of its ends. Furthermore the portion to one side of this plane is a graph over some domain Ω contained in the horizontal plane. Since our surface has genus 0, the domain Ω is simply connected. It follows that the vertical axis of symmetry meets our surface in a point $\tilde{p}$ and its mirror image under the horizontal symmetry as in Figure 2. For $k \geq 3$ these two points must be umbilics. We claim these are the only umbilics on the surface, and each is of index $(2-k)/2$.

Before proving this claim, we use it obtain the bound on the length of the great circle arc: The boundary contour of the fundamental domain of the surface is made up of planar curvature arcs, and the principal curvature on these is different from 1 except at $\tilde{p}$. Since we know from the asymptotics that the principal curvatures of the t- and s-arc change sign, their curvatures must be smaller than 1. But the mean curvature is 1, so the curvature of the r- and l-arcs must be larger than 1. Since the total turn of the normal is $\pi/2$ along the planar r- and l-arcs, their lengths must be bounded:

$$r, l < \pi/2.$$

To prove the claim, we note that the umbilic points and their indices correspond to the zeros of the holomorphic quadratic (Hopf) differential Q associated to any CMC surface. A zero of Q of order n gives an umbilic of index $-n/2$. The total order of Q on a closed surface of genus g equals $4g-4$. However, our complete surfaces are conformally closed surfaces with k punctures, and near each puncture

Q has a double pole, so the total of zeros is $4g-4+2k$ instead. On a surface of genus zero, this means the total index of umbilics is then $2-k$ (the Euler number of the surface). But the k-fold symmetry implies the index of each of the two umbilics is at most $(2-k)/2$, and so must equal $(2-k)/2$ as claimed.

The statements on the quadrilateral follow from the Hopf fields of the contour and Lemma 2. □

In [G] we solved Plateau's problem for the degenerate spherical triangles given by the previous lemma.

Theorem 7. *Any (Alexandrov embedded) dihedrally symmetric k-unduloid is contained in the family given in* [G].

Proof. The previous lemma shows that the associated boundary contour is of the type considered in [G]. If there was any surface different to our family, then it would lead to another spherical minimal surface bounded by the same contour.

By Alexandrov embeddedness the total turn of the normal along the boundary arcs is given by the real numbers $0, \pi/2, 0$.

We now use the foliation described in [G] to show uniqueness of the minimal surfaces bounded by the degenerate Lawson triangles.

```
uups.  I have to think about this, hopefully it will work out
```

□

3. Rectangular surfaces

In the CMC patch for a rectangular surface there is one planar curvature line running from one end to the other, see Figure 3.1. Thus two opposite geodesic rays of the associated patch match to a line. The other pair of rays meets at a right angle in a point $p \in \mathbb{S}^3$ as the curvature lines of the CMC patch do.

The associated contour thus consists of two geodesic rays and one line. It is a simplification to truncate its ends. For this we use the pair of perpendiculars provided by Lemma 2; we truncate at the necks, i.e. the truncated arcs have the shorter set of lengths

$$0 < l_1, l_2 \leq \pi/4. \tag{11}$$

The resulting pentagon, with the truncated line of length s, two truncated rays of lengths t_1, t_2, and two connecting arcs of lengths l_1, l_2, is a right-angled pentagon denoted $\Gamma(t_1, l_1, s, l_2, t_2)$.

To reduce the spherical trigonometry of these pentagons to the quadrilaterals of Subsection 1.3 we determine the Hopf fields of the pentagons. We start at the

intersection point $\tilde{p}$ of the geodesic rays. The Hopf fields, compare Figure 3.2 are then A, $-C$, $-B$, $-A$, and C, where $-B$ runs from one end to the other. Here the $-C$ and $-A$ fields of the arcs capping the ends, are defined up to sign by the fact that they are perpendicular to their adjacent arcs; the sign follows from asymptotics of the ends. We refer to such a pentagon, whose lengths satisfy (11) as a *pentagon for rectangular surfaces*. The main geometric observation for these pentagons is (see Figure 3):

Lemma 8. (i) *Two Lawson quadrilaterals* $\Gamma_1(l_1, t_1, r, s_1; \beta)$ *and* $\Gamma_2(l_2, t_2, r, s - s_1; \pi/2 - \beta)$ *with angle* $0 < \beta < \pi/2$ *can be glued together along their* r *arcs to form a pentagon with Hopf fields for rectangular surfaces* $\Gamma(t_1, l_1, s, l_2, t_2)$.
(ii) *On the other hand, a pentagon with sufficiently large* s, t *and satisfying* (11) *can be decomposed into two Lawson quadrilaterals.*

Proof. (i) If the two quadrilaterals are glued along their arcs of lengths r in such a way that the two non-right angles face each other and are contained in the same tangent plane, a rightangled pentagon is formed. Moreover, this pentagon has the correct Hopf fields.

(ii) Given the pentagon we define the diagonal as the geodesic arc orthogonal to the geodesic containing the $-B$ arc, which meets the intersection point p of the C and A arc, and which has length smaller than $\pi/2$. By orthogonality its Hopf field must be of the form $\sin\beta\, A - \cos\beta\, C$ with respect to an orientation as in Figure 3. Note that $0 < \beta < \pi$ for a non-degenerate pentagon.

Then the Hopf fields of the two quadrilaterals imply that the quadrilaterals are of Lawson type. This is also evident from the fact that the arcs l_1 and l_2 cap off quarter ends. □

We will see below that it is not necessary to require that s and t are large.

We now analyse the pentagons via the two quadrilaterals the lemma provides. Let us remark that the family of dihedrally symmetric 4-unduloids constructed in [G] satisfy $0 < \rho \leq 1/4$. Thus they lead to symmetric pentagons $\Gamma(l, t, s, t, l)$ with $0 < l \leq \pi/8$; these decompose into two equal Lawson quadrilaterals $\Gamma(l, t, r, s/2; \pi/4)$ as given by Lemma 4(i). For the general case we take two different quadrilaterals but we can prove that $l_1 + l_2 \leq \pi/4$ still holds.

Proposition 9. *There exists a continuous 1-parameter family of pentagons*

$$\mathcal{G} = \{\Gamma(t_1, l_1, s, l_2, t_2) \mid 0 < l_1, l_2 \text{ and } l_1 + l_2 \leq \pi/4,\ 0 < t_1, t_2, s < \pi/2\},$$

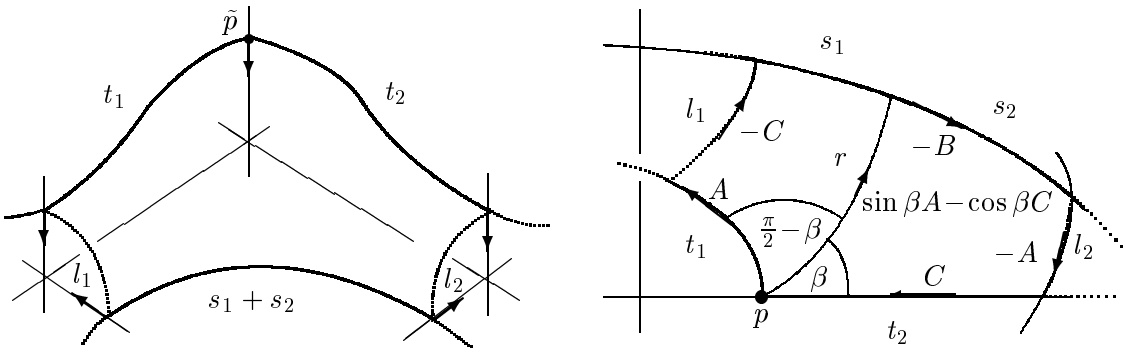

FIGURE 3. Generating CMC patch for a rectangular surface, and spherical boundary polygon of associated spherical minimal surface. The truncation of the patches by two arcs is indicated with dotted lines; an extra arc in the spherical contour gives the decomposition into two quadrilaterals.

with the Hopf fields for rectangular surfaces. For each pair of $l_1, l_2 > 0$ *with* $l_1+l_2 < \pi/4$ *the family contains exactly two different pentagons, while for* $l_1+l_2 = \pi/4$ *there is only one such pentagon.*

Proof. We determine a quadrilateral $\Gamma_1(l_1, t_1, r, s_1; \beta)$ with angle $0 < \beta < \pi/2$ and all edgelengths in $(0, \pi/2)$ as follows. We take $0 < l_1 \leq \pi/4$ and r with $l_1 \leq r \leq \pi/2 - l_1$ as parameters. Then (8) (with $l = l_1$) gives

$$\cos^2\beta = \frac{\cos^2 2l_1 - \cos^2 2r}{\sin^2 2r} \tag{12}$$

and we obtain a $\beta \geq 2l_1$. Since $l_1 \leq r$ the numerator of (12) is positive, and the fraction is at most 1, so that we can choose $\beta < \pi/2$. Then Lemma $4(i)$ gives existence of a family of quadrilaterals $\Gamma_1(l_1, t_1, r, s; \beta)$ with $0 < t < \pi/2$ and $0 < s < \beta < \pi/2$ as in (7) and (6). These quadrilaterals depend continuously on the parameters r and l_1.

With r and β fixed, we now construct another quadrilateral $\Gamma_2(l_2, t_2, r, s - s_1; \pi/2 - \beta)$. According to (8) and Lemma $4(i)$ there is such a quadrilateral with $0 < l_2 \leq \pi/4$ determined by

$$\cos^2 2l_2 = \cos^2(\pi/2 - \beta)\sin^2 2r + \cos^2 2r, \tag{13}$$

and $0 < t_2 < \pi/2$ and $s - s_1 < \pi/2 - \beta$ given by (7) and (6). Consequently, the quadrilaterals Γ_2 form a family which is continuous in (l_1, r). By Lemma 8 this gives a pentagon for rectangular surfaces.

We now want to show that any pair l_1, l_2 with $l_1 + l_2 \leq \pi/4$ is attained, such that there are two different pentagons for $l_1 + l_2 < \pi/4$, and one if equality holds.

For this we consider the extremal choices of r. If $r \to l_1$ then by (12) $\beta \to \pi/2$, and thus by (13) $l_2 \to 0$. On the other hand, for $r = \pi/4$, (12) implies $\beta = 2l_1$, and from (13) we conclude $2l_2 = \pi/2 - 2l_1$. By continuity we obtain that for given l_1 a choice of r in the lower interval $(l_1, \pi/4]$ gives all $l_2 \in (0, \pi/4 - l_1]$. Taking r-derivatives of (12) and (13) it is elementary to see that, for given l_1, the function $l_2(r)$ is strictly monotonic. Thus each l_2 in $(0, \pi/4 - l_1]$ is taken exactly once, and in particular $l_1 + l_2 \leq \pi/4$. We denote

The upper r-interval $[\pi/4, \pi/2 - l_1)$ also yields quadrilaterals $\Gamma_2(l_1, r)$ with $l_2 \in (0, \pi/4 - l_1]$. This follows with the same arguments since the limit $r \to \pi/2 - l_1$ is analogous to $r \to l_1$. □

There are further families of pentagons with rectangular Hopf fields. Clearly we can extend (i) s and t_1 by π or any integer multiple of π, or (ii) do the same with s and t_2. Finally, (iii) we can extend any of s, t_1, t_2 by integer multiples of 2π. This way all pentagons of rectangular type are obtained.

Lemma 10. *All pentagons with rectangular Hopf fields are generated from the family $\mathcal{G}$ by the substitutionns (i), (ii), or (iii).*

Proof. Given a pentagon, we arrive at two Lawson quadrilaterals Γ_1 and Γ_2 as in Lemma 8. It follows from Lemma 5 that these quadrilaterals are uniquely determined by r and l_1 up to the ambiguity given by (i) to (iii). □

Lemma 11. *The family $\mathcal{G}$ forms a maximal continuous family.*

Proof. We have to show that all non-degenerate pentagons of rectangular type in a sufficiently small neighbourhood of $\mathcal{G}$ are actually in $\mathcal{G}$.

Let us consider a path $\Gamma(\sigma)$, $\sigma \in [0, 1]$, of pentagons of rectangular type, such that $d(\Gamma(\sigma), \Gamma(0)) \to 0$ and $\Gamma(\sigma) \in \mathcal{G}$ only for $\sigma = 0$.

We decompose the pentagon $\Gamma(\sigma)$ into two quadrilaterals by Lemma $8(ii)$. The diagonal depends continuously on σ. For $\sigma = 0$ the diagonal meets the opposite $-B$ arc at an interior point, and this extends to small $\sigma > 0$, too. Furthermore by continuity we can assume $0 < l_1, t, r, s < \pi/2$ for small σ, and thus, by Lemma $4(i)$, the quadrilateral $\Gamma_1(l_1, r)$ of the proof of the previous proposition is unique. Similarly, this determines a unique $\Gamma_2(l_1, r)$, and it follows that the quadrilaterals arise in the construction of the previous proposition. Hence $\Gamma(\sigma)$ is contained in $\mathcal{G}$ for small σ, in contradiction to our assumption. □

Taking the proposition and the previous theorem together we we arrive at our main statement for the rectangular surfaces.

Theorem 12. *There is a maximal continuous 1-parameter family of associated spherical boundary contours for rectangular surfaces, with the four necksizes of the ends $\rho_1 = \rho_3$ and $\rho_2 = \rho_4$ satisfying*

$$\sum_{i=1}^{4} \rho_i \leq 1. \tag{14}$$

If the necksizes satisfy the strict inequality there are two different such contours, and one for equality.

We would also like to mention a consequence on *doubly periodic* CMC *surfaces of rectangular type*. By this we mean surfaces whose fundamental domain is a pentagon with rectangular Hopf fields, i.e. no truncation is involved. These surfaces have a planar rectangular lattice, whose parameters are related to the lengths of t_1, t_2, and s. For these surfaces we have to give a different definition of necksize. For our purposes it is reasonable to define the necksize ρ via the spherical distance of the meridians. This length is reflected in the length of the symmetry curve intersecting a handle: the necksize is thus the length l of the symmetry curve divided by 2π, i.e. $\rho := \min(l/2\pi, 1 - l/2\pi)$; the minimum arises since the symmetry curve sits can sit on a neck or on a bubble.

Theorem 13. *There are countably many maximal continuous 1-parameter families of associated spherical boundary contours for doubly periodic rectangular surfaces. In each family, the four necksizes of the handles $\rho_1 = \rho_3$ and $\rho_2 = \rho_4$ satisfy* (14) *with two different contours for strict inequality and just one for equality.*

Proof. If $\Gamma(t_1, l_1, s, l_2, t_2)$ is a pentagon with rectangular Hopf fields then so is $\Gamma(t_1 + m\pi, l_1, s + (m+n)\pi, l_2, t_2 + n\pi)$ for $m, n \in \mathbb{N}$. `some more things` □

The main theorem of this section follows. `Check the statement for the Kapouleas surfaces, for the others it is clear.`

Theorem 14. *Let $\mathcal{M}$ be a connected component of the moduli space of the rectangular* CMC *surfaces containing surfaces of Kapouleas, Brauckmann, or Berglund. The four neck radii $\rho_1 = \rho_3$, $\rho_2 = \rho_4$ for each surface in $\mathcal{M}$ satisfy* (14).

Remark: We believe there is only one component of the Alexandrov embedded rectangular surfaces. However, it is not even clear that Kapouleas' surfaces are all in the same connected component (see Remark 4.6 of [Kp]). All we know on the number of components is that the number containing surfaces with necksize at least $\epsilon > 0$ must be finite; this follows from the curvature and area bounds of [KK]. Note that our spherical contours could bound many minimal surface patches. This could give rise to many connected components of the moduli space.

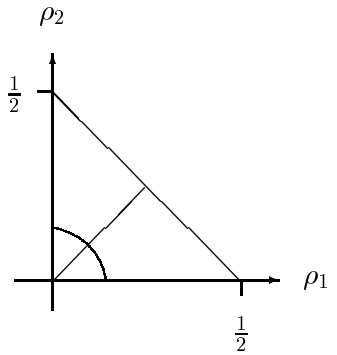

FIGURE 4. Schematic diagram of the moduli space for the rectangular surfaces. Our associated boundary contours give a two-sheeted covering of the triangle defined by $\rho_1, \rho_2 > 0$ and $\rho_1 + \rho_2 < 1/2$. Existence is known in a dense subset of a neighbourhood of the origin by Kapouleas (on one sheet), on the diagonal by one of the authors (on both sheets), and on the line $\rho_1 + \rho_2 = 1/2$ in some neighbourhood of the coordinate axes by Berglund.

The relation (14) can be expressed in terms of the force. The force w is quadratic in the minimal radius ρ, in fact $1/2 - w/\pi = 2(\rho - 1/2)^2$ and hence (14) gives the quadratic equation on w_1 and w_2

$$\sqrt{\frac{1}{4} - \frac{w_1}{2\pi}} + \sqrt{\frac{1}{4} - \frac{w_2}{2\pi}} \geq \frac{1}{2}.$$

Similarly we obtain an equation for the radii quotients a_1, a_2: $a_1/[a_1 + 1] + a_2/[a_2 + 1] \leq 1/2$. Comparing these equivalent formulas to (14) it seems that the minimal Delaunay radius is the appropriate way to parameterize the moduli space for the present problem.

4. Isosceles surfaces

Trigonometry. For the isosceles surface a fundamental domain comprises a quarter end and a half end. Since the ends are asymptotically Delaunay [KKS], by balancing their axis are contained in a plane, and they meet in a point. We remark that a similar statement applies to the general three-ended surfaces, and can be proved using torques (see [K1]). Thus arms and stem of these Y-shaped surfaces enclose a well-defined angle. We choose α to be this angle as indicated in Figure 1; that is $\alpha = 0$ means that the arms straightly extend the stem to form a I, whereas for $\alpha = \pi/2$ the surface looks like a T. The balancing formula implies that, for a surface with embedded ends,

$$\alpha \in (0, \pi/2).$$

CMC surfaces with $\pi/2 < \alpha < \pi$ exist in the non-Alexandrov-embedded class, for instance with either stem or arms nodoid ends [Kp].

The fundamental patch is again bounded by a geodesic line and two rays. As before the result on the asymptotics of the ends allows to truncate the infinite contour in order to obtain a finite pentagon.

Starting with the saddle point p (see Figure 5) the Hopf fields of a pentagon can be seen to be $-B$, $\cos\alpha\, A - \sin\alpha\, C$, $-B$, $-A$, C. We call a pentagon with such Hopf-fields a *pentagon for isosceles surfaces*, and denote it with its five lengths $\Gamma(b, r, s-b, l, t)$. We can require

$$0 < l \le \frac{\pi}{4} \qquad \text{and} \qquad 0 < r \le \frac{\pi}{2}, \tag{15}$$

if we truncate the contour with the shorter geodesics, i.e. we cap the ends at the necks not at the bubbles. Similar to the rectangular case, the main idea is to reduce the trigonometry of the pentagon to a Lawson quadrilateral.

Lemma 15. *(i) A Lawson quadrilateral $\Gamma_1(l, t, r, s; \pi/2 - \alpha + 2b)$ and a Clifford rectangle $\Gamma_2(b, r)$ can be glued together to form a pentagon $\Gamma(b, r, s-b, l, t)$ for isosceles surfaces provided $s > b$.*
(ii) Conversely, a pentagon satisfying (15) and $k\pi < s - b, t < (k+1)\pi$ for sufficiently large $k \in \mathbb{Z}$ can be decomposed into a Lawson quadrilateral and a Clifford rectangle as in (i).

Proof. (i) Taking a Lawson quadrilateral, and glueing a Clifford rectangle along the r-arc, such that the s arc is shortened yields a pentagon for isosceles surfaces.
(ii) We consider an arc perpendicular to the geodesic line and passing through the point p. The arc can be constructed explicitely as follows. Since both arcs running along the half end have the same $-B$ Hopf field they have a continuous set of perpendiculars, which are all Clifford parallel to the r-arc. Thus the diagonal is a Clifford parallel to the r-arc in distance b. Its Hopf field, in the orientation indicated in Figure 5 is $\cos(\alpha - 2b)\, A - \sin(\alpha - 2b)\, C$. We have to go the same distance b on both $-B$ arcs to obtain the Clifford rectangle of the r-arc and the diagonal; this means that the diagonal does not meet the opposite $-B$ arc, but an extension of forms the side of the rectangle.

Writing the Hopf field of the diagonal in the form $\sin(\pi/2 - \alpha + 2b)\, A - \cos(\pi/2 - \alpha + 2b)\, C$ we see that the other quadrilateral formed has a non-right angle

$$\beta := \frac{\pi}{2} - \alpha + 2b$$

at p. It is clearly a Lawson quadrilateral, since the $-A$ arc caps off a quarter end. □

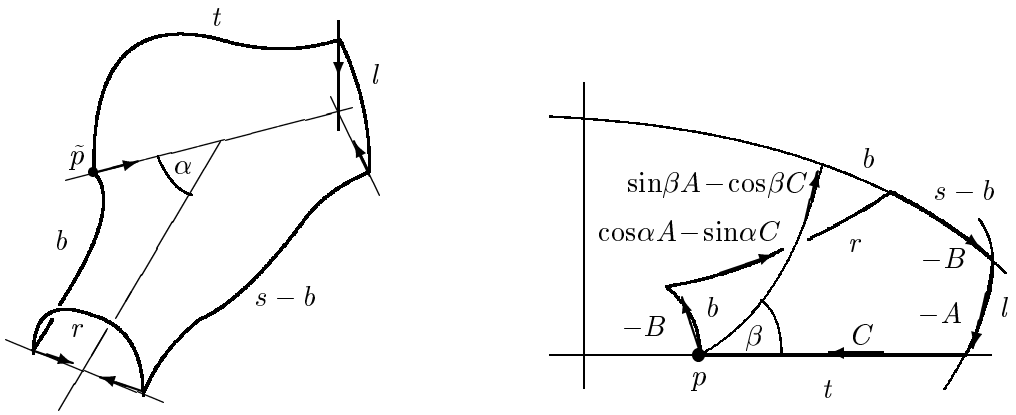

FIGURE 5. Generating CMC patch for an isosceles surface, and spherical boundary polygon of associated spherical minimal surface.

We want to investigate how the length l of the arc capping the quarter end (stem of Y) relates to the length r of the arc capping the half end (arms of Y). For the Lawson quadrilateral $\Gamma_1(l, t, r, s; \pi/2 - \alpha + 2b)$ the following relation is obtained from (8)

$$\cos^2 2l = \sin^2(\alpha - 2b) \sin^2 2r + \cos^2 2r. \tag{16}$$

Not every pentagon with the Hopf fields for isosceles surfaces actually leads to an isosceles surface: If there is a minimal surface spanned by the pentagon then the two boundary rays of the half end (arms) of the associated CMC surface must be contained in parallel planes. To generate an isosceles surface upon reflection these arcs have to be in parallel planes. Thus a period problem must be solved.

4.1. **Balancing.** To solve the period problem we use the balancing formula. This statement should be taken with care: we do not give an existence proof, and in particular we do not show that the pentagons which the balancing formula admits span minimal surfaces with vanishing periods. Thus technically we discuss a further necessary condition, which reduces the number of free parameters to the correct number: one. Only in the case of the symmetric family, $\alpha = \pi/3$, it can be checked that the condition we obtain from balancing is satisfied by the surfaces with closed periods.

In the following we take the index S for the stem and A for the arms. The balancing formula (10) gives

$$|f_S| = 2 \cos\alpha \, |f_A|.$$

Thus (9) gives the relation $2\pi\rho_S(1-\rho_S) = 2\cos\alpha\, 2\pi\rho_A(1-\rho_A)$ for minimal radii ρ_S and ρ_A. These radii are $2\pi\rho_S = 4l$ and $2\pi\rho_A = 2r$ in terms of the arclengths of the pentagon. We obtain

$$l(\pi - 2l) = \cos\alpha\, r(\pi - r). \tag{17}$$

Solving this quadratic equation (using (15)) for l we arrive at the following statement.

Lemma 16. *Assume that the geodesics of the half end for a fundamental spherical patch of a balanced isosceles surface have perpendiculars of length r and $\pi - r$. Then the geodesics of the quarter end have perpendiculars of length $0 < l \leq \pi/4$ and $\pi/2 - l$, where l satisfies*

$$l = \frac{\pi}{4} - \sqrt{\frac{\pi^2}{16} - \cos\alpha\, \frac{r(\pi - r)}{2}}. \tag{18}$$

In particular, (18) has only a solution for those $0 \leq r \leq \pi/2$ which are in the interval

$$I(\alpha) := \begin{cases} \left[0, \frac{\pi}{2}\left(1 - \sqrt{1 - \frac{1}{2\cos\alpha}}\right)\right] & \text{for} \quad 0 < \alpha \leq \frac{\pi}{3} \\ \left[0, \frac{\pi}{2}\right] & \text{for} \quad \frac{\pi}{3} \leq \alpha < \frac{\pi}{2} \end{cases} \tag{19}$$

We now want to construct a family of pentagons satisfying (16) and (18). Eliminating r from the equations means that (r, b) are a zero of the function

$$f(r,b) := \sin^2(\alpha - 2b)\sin^2 2r + \cos^2 2r - \sin^2\left(2\sqrt{\frac{\pi^2}{16} - \cos\alpha\, \frac{r(\pi - r)}{2}}\right).$$

The function f is defined on $I(\alpha) \times \mathbb{R}$.

From [Kp] it follows that isosceles surfaces with small weights exist, and we want to continue their branch in the moduli space. It is not known that the Kapouleas isosceles surfaces form indeed a continuous family. Still, the associated boundary contour for the degenerate limit, when the neck sizes tend to 0, is uniquely defined, and, capping the ends off at the central bubble, we call it a *degenerate Kapouleas pentagon.* It has the following trigonometric data: The ends have $l = r = 0$, the geodesic line has length $s - b = \pi - \alpha$, the rays length $t = \pi$, $b = \alpha$.

Proposition 17. *For each $0 < \alpha < \pi/2$ there is a continuous 1-parameter family of pentagons satisfying* (16) *and* (18). *This family extends the degenerate*

Kapouleas pentagons and is a maximal continuous family with non-zero edge-lengths. These pentagons attain all r admissable in

$$0 < r \leq R(\alpha) := \pi \frac{1-\cos\alpha}{2-\cos\alpha}. \tag{20}$$

For strict inequality there are two such pentagons in the family, and, if $\alpha \neq \arccos(2/3)$, for equality just one . For $\alpha = \arccos(2/3)$ there is a one-parameter family of contours satisfying $r = R(\arccos(2/3)) = \pi/2$.

Proof. We want to establish solutions $f(r,b) = 0$ for all $0 < r \leq R(\alpha)$. Let us first of all show that $f(r,b)$ is defined for all $0 < r \leq R(\alpha)$, $b \in \mathbb{R}$. We have to show that

$$[0, R(\alpha)] \subset I(\alpha). \tag{21}$$

Since $R(\alpha) < \pi/2$ this is clear for $\alpha \geq \pi/3$. For $0 < \alpha < \pi/3$ (21) is equivalent to

$$1 - 2\,\frac{1-\cos\alpha}{2-\cos\alpha} \geq \sqrt{1 - \frac{1}{2\cos\alpha}}.$$

The left hand side is equal to $[2-\cos\alpha-(2-2\cos\alpha)]/[2-\cos\alpha] = \cos\alpha/[2-\cos\alpha]$. Since this is positive, squaring gives the equivalent inequality

$$\frac{\cos^2\alpha}{\cos^2\alpha - 4\cos\alpha + 4} \geq \frac{\cos\alpha - \frac{1}{2}}{\cos\alpha},$$

or $\cos^3\alpha \geq \cos^3\alpha - \frac{9}{2}\cos^2\alpha + 6\cos\alpha - 2$. This inequality is valid since

$$-\frac{9}{2}\cos^2\alpha + 6\cos\alpha - 2 = -\left(\frac{3}{\sqrt{2}}\cos\alpha - \sqrt{2}\right)^2 \leq 0,$$

and holds with equality for $\cos\alpha = 2/3$.

We want to find a branch of zeros $(r, b(r))$ for $0 < r < R(\alpha)$. We establish $b(r)$ in the interval $(\alpha/2 - \pi/4, \alpha/2)$, which means that $0 < \beta < \pi/2$. This first branch of solutions will be extended by a second branch of zeros below. To apply the implicit function theorem we show three facts:
(i) $\frac{\partial f}{\partial b} < 0$ on $D := (0, R(\alpha)) \times (\alpha/2 - \pi/4, \alpha/2)$,
(ii) $f(r, \alpha/2 - \pi/4) > 0$ for $0 < r < R(\alpha)$, and
(iii) $f(r, \alpha/2) < 0$ for $0 < r < R(\alpha)$.

The derivative

$$\frac{\partial f}{\partial b} = -2\sin(2\alpha - 4b)\sin^2 2r \tag{22}$$

is negative on D which proves (i). We now prove (ii). Since $\sin^2(\alpha - 2(\alpha/2 - \pi/4)) = 1$ we have $f(r, \alpha/2 - \pi/4) = \sin^2 r + \cos^2 r - \sin^2\left(2\sqrt{\frac{\pi^2}{16} - \cos\alpha\frac{r(\pi-r)}{2}}\right) = \cos^2(2\sqrt{\dots})$. Clearly this is non-negative; it is in fact positive for $0 < r \in I(\alpha)$.

To prove (iii) amounts to a further elementary calculation. $f(r, \alpha/2) < 0$ is equivalent to

$$\sin^2\left(\frac{\pi}{2} - 2r\right) < \sin^2\left(2\sqrt{\frac{\pi^2}{16} - \cos\alpha\frac{r(\pi-r)}{2}}\right).$$

Since $0 < 2\sqrt{\dots} < \pi/2$ and $-\pi/2 < \pi/2 - 2r < \pi/2$ this is equivalent to

$$\left|\frac{\pi}{4} - r\right| < \sqrt{\frac{\pi^2}{16} - \cos\alpha\frac{r(\pi-r)}{2}}.$$

Squaring yields

$$\frac{\pi^2}{16} - \frac{r(\pi-2r)}{2} < \frac{\pi^2}{16} - \cos\alpha\frac{r(\pi-r)}{2},$$

which is equivalent to $\pi - 2r > \cos\alpha(\pi - r)$ or $\pi(1 - \cos\alpha) > (2 - \cos\alpha)r$. Thus we arrived at our assumption (20).

This gives a differentiable function $b(r)$ for $0 < r < R(\alpha)$, which is unique in D by (i).

We construct a second branch. It can be obtained from the first one by means of the substitution $b \mapsto \alpha - b$. Then $\alpha - 2b \mapsto 2b - \alpha$, and, in particular, f is invariant under this substitution. Thus if $(r, b(r))$ is a zero of f then so is $(r, \alpha - b(r))$. Since $0 < \beta < \pi/2$ on the first branch we have $\pi/2 < \beta < \pi$ on the second branch.

We patch the two branches together to determine a continuous 1-parameter family of quadrilaterals, which will give the desired pentagons. We discuss different cases.

- First branch, i.e. $0 < \beta < \pi/2$: We find an $0 < l \leq \pi/4$ satisfying (16), and the two remaining lengths $0 < t, s < \pi/2$ for a continuous family of quadrilaterals $\Gamma(l, t, s, r; \beta)$ by (7) and (6). To discuss the limiting behaviour (L1) of $r \searrow 0$, and (L2) of $r \nearrow R(\alpha)$ we need to distinguish the following cases:
  - $0 < r < \pi/4$: Under these assumptions an l solves (16) with

$$0 < l < r < \pi/4. \tag{23}$$

We have $0 < t < r < \pi/4$, since (7) gives that $\tan 2t > 0$. Furthermore, by (6)

$$0 < s < t < r < \pi/4. \tag{24}$$

Consider the limit (L1) with $r \searrow 0$. From (23) and (24) follows $l, s, t \searrow 0$, so that all lengths tend to 0. For later use we want to show that (0,0) is the limiting zero, that is $r \searrow 0$ gives $\beta \searrow \pi/2 - \alpha$, or, equivalently $b \searrow 0$. This is proved by writing $f(b, r)$ for small r as

$$f(b, r) = 4r^2 \left(\cos^2\alpha - \cos^2(\alpha - 2b)\right) + O(r^4). \tag{25}$$

On the other hand we consider the limit (L2) with $r \nearrow R(\alpha) < \pi/4$, or equivalently $\beta \nearrow \pi/2$. By (7) it follows that $t \searrow 0$, and (24) gives $s \searrow 0$.

* $\pi/4 < r < R(\alpha)$: In this case (7) gives
$$\frac{\pi}{4} < r < t < \pi/2.$$
The limiting quadrilaterals for (L2) with $\beta \nearrow \pi/2$ have $t \nearrow \pi/2$ by (7), and $s \nearrow \pi/2$ by (6).
* $r = \pi/4$: This condition gives $t = \pi/4$ by (7).

- Second branch, i.e. $\pi/2 < \beta < \pi$: Again we find an $0 < l \leq \pi/4$ satisfying (16), and the two remaining lengths $\pi/2 < t, s < \pi$ for a continuous family of quadrilaterals $\Gamma(l, t, s, r; \beta)$ are determind by (7) and (6). These quadrilaterals can also be obtained from the first branch by the substitution

$$(l, r, s, t; \beta) \mapsto (l, r, \pi - s, \pi - t; \pi - \beta). \tag{26}$$

Similar to the limits before, we consider the limit behaviour (L3) of $r \nearrow R(\alpha)$, and (L4) of $r \searrow 0$.

* $0 < r < \pi/4$: The substitution (26) transforms (24) to

$$0 < \pi - s < \pi - t < r < R(\alpha) < \pi/4. \tag{27}$$

In particular (26) gives the limit (L4): we obtain $s, t \nearrow \pi$, $l \searrow 0$ for this limit, and $b \nearrow \alpha$. Therefore we recognize (L4) as the Kapouleas limit. The limit (L3) $\beta \searrow \pi/2$ is similar to (L2); we have $s, t \to \pi$.
* $\pi/4 < r < R(\alpha)$: The limit (L3) has $s, t \searrow \pi/2$.
* $r = \pi/4$: This condition gives $t = 3\pi/4$ by (7).

- Maximal $r = R(\alpha)$: A zero of $f(R(\alpha), b)$ is $b = \alpha/2$, which is unique in $(-\alpha/2 - \pi/4, \alpha/2 + \pi/4)$.
* $R(\alpha) < \pi/4$: (16) gives $\cos^2 2l = \cos^2 2r$, and by (15) $l = R(\alpha)$. We find quadrilaterals with $s, t = \pi$ by Lemma 4(iv).

  - $R(\alpha) = \pi/4$: (16) gives $l = \pi/4$, and there is a one-parameter family of quadrilaterals of the form $\Gamma(\pi/4, t, \pi/4, t; \pi/2)$ with $t > 0$. These are in fact Clifford rectangles $\Gamma(\pi/4, t)$, and the one parameter family is related to the fact that a surface with a cylinder end does not have a discrete set of perpendiculars.
  - $R(\alpha) > \pi/4$: The quadrilaterals satisfy $l = \pi/2 - R(\alpha)$ by (16) and (15), so that $t = s = \pi/2$ by Lemma 4(*iii*).

It remains to patch the continuous families together at $r = R(\alpha)$. Again we distinguish cases according to how α relates to

$$0 < \alpha_0 := \arccos 2/3 < \pi/2.$$

- $R(\alpha) < \pi/4 \Leftrightarrow 0 < \alpha < \alpha_0$: The limits (L2) and (L3) do not match continuously. However, if we extend the s- and t-arcs of the first arc by π, then all lengths are continuous and agree with the quadrilaterals for $r = R(\alpha)$.
- $R(\alpha) = \pi/4 \Leftrightarrow \alpha = \alpha_0$: To discuss the limits (L2) and (L3) we need to consider the equations up to first order. First we consider (L2), i.e. $l, r \nearrow \pi/4$. From (17) we obtain

  $$\frac{6}{\pi}\left(\frac{\pi}{4} - l\right)^2 = \frac{\pi}{4} - r + o(\frac{\pi}{4} - r).$$

  This expression can be substituted into (16) to give the expression

  $$\beta(l) = \frac{\pi}{2} + 2(\frac{\pi}{4} - l) + o(\frac{\pi}{4} - l).$$

  This can be used to calculate the limiting value for t with (7), $\tan 2t = \cos\beta \tan 2r$: since β is $(\pi/4 - l)$ in first order, but $\cos 2r$ only $(\pi/4 - l)$ in second order it follows that $\tan 2t \nearrow \infty$. Therefore, the limit of t in (L2) is $\pi/4$, and this gives $s \nearrow \pi/4$. Similarly for the limit (L3) where $s, t \searrow 3\pi/4$. The quadrilateral with $r = R(\alpha_0) = \pi/4$ is special. Since $l = \pi/4$, the stem has a cylinder end. In particular there is a continuous set of perpendiculars, i.e. we can choose any length for $s = t$. To make the family of quadrilaterals continuous at $r = R(\alpha)$ we can vary $s = t$ from $\pi/4$ to $3\pi/4$ to join the limits (L2) and (L3).
- $R(\alpha) > \pi/4 \Leftrightarrow \alpha_0 < \alpha$: The family of quadrilaterals obtained above is continuous in this case.

Replacing the r-arc of the quadrilaterals by its Clifford parallel in distance $b(r)$, and joining it to the t-arc with an arc of length b, as well as shortening the s-arc by b gives the desired pentagons, whose lengths satisfy (18) and (16).

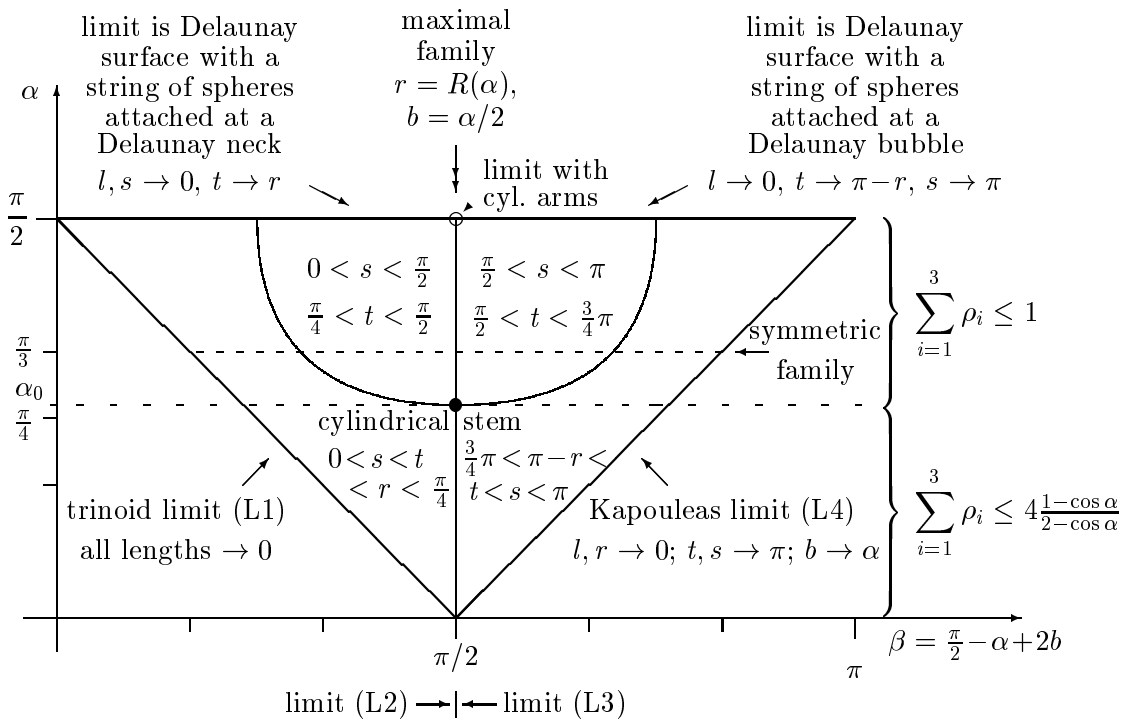

FIGURE 6. Schematic diagram of the submoduli space for isosceles surfaces. Boundary contours for these surfaces exist inside the bold triangle and degenerate on its boundary as indicated. Both neck-sizes are symmetric to the line $\beta = \pi/2$ and attain their maximum on this line. Existence is only proved for the symmetric family [G] and in a neighbourhood of the Kapouleas boundary [Kp].

`It remains to show that our pentagons form a maximal continuous family. Should be similar to the rectangular case.` □

Remark: (i) The above 1-parameter families do not yield a continuous 2-parameter family of pentagons $\mathcal{F}(\alpha, r)$. Clearly a discontinuity arises at $(\alpha_0, R(\alpha_0)) = \pi/4)$. Instead of our continuous families for each α it is helpful to consider the original choice of lengths obtained in the proof (no extension of the t- and s-arcs on the first branch of (i)): the disconinuity is then located on the arc $\{(\alpha, r) | 0 < \alpha \le \alpha_0, r = R(\alpha)\}$. It should be viewed as a discontinuity which is in our description of the moduli space of the isosceles surfaces, not in these surfaces themselves. Indeed, the definition of the lengths s, t and b is arbitrary, while the only parameters on the surface are the continuous parameters r and l. Even so there is a mathematical observation for the moduli space to make: a curve in the moduli

space $\mathcal{F}(\alpha, r)$ which winds once around the point $(\alpha_0, \pi/4)$ will create (or remove) one bubble on the stem. Indeed, the fact that we have to extend s, t by π when going from (L2) to (L3) in case (i) means that we add a bubble on the stem.

(ii) The *maximal* family with the maximal weights for each α is not continuous at α_0, but can easily be altered to become continuous. For this, we have to relax the requirement (15): if we admit to vary l in the larger interval $(0, \pi/2]$ then the maximal family satisfies:

$$t = \frac{\pi}{2},\ \ l = \frac{\pi}{2} - R(\alpha),\ \ s - b = \frac{\pi}{2} - \frac{\alpha}{2},\ \ r = R(\alpha),\ \ b = \frac{\alpha}{2}$$

This means, that for $\alpha < \alpha_0$ we "cut" the surface at the bubble, for $\alpha > \alpha_0$ at the necks. Of course for continuity of the surfaces (in a fixed compact set) this does not matter.

We expect that for all pentagons in the family the Plateau problem can be solved, so that the family corresponds to a component of the moduli space. However, to solve the Plateau problems needs barriers and this is technically difficult. Therefore the statement we can make on the CMC surfaces is as follows:

Theorem 18. *The connected component of the moduli space of the iscosceles surfaces containing Kapouleas surfaces satisfies*

$$\rho_1 + \rho_2 + \rho_3 \ \ \leq \min\left(1, 4\,\frac{1-\cos\alpha}{2-\cos\alpha}\right). \tag{28}$$

For $\alpha_0 = \arccos\frac{2}{3} \approx 48.2^\circ$ we have $R(\alpha_0) = \pi/4$. Thus the minimum on the right hand side of (28) is 1 for $\alpha_0 \leq \alpha < \pi/2$, but smaller for $0 < \alpha < \alpha_0$.

`All other statements as in the rectangular case`

A preliminary remark on *rhombic* surfaces: Assume that there is a spherical minimal surface that bounds contours which are only truncated along the l arc. Does reflection of the associated CMC contour lead to a rhombic surface? This does not seem to be the case. Note that for the condition (10) we used to select a contour that bounds a surface with (presumably) closed periods we needed the asymptotics of the ends. Namely we assumed that the reflected arcs form round circles, so that we could compute their weights with (9). This does not imply that the period problem is solved for the truncated contours. The following facts support this view:
(i) For $\alpha = \pi/4$ the rhombic surface is the 4-ended symmetric surface of [G], so that the family satisfies $\sum_1^4 \rho_i \leq 1$. On the other hand the isosceles family $\mathcal{F}(\pi/4)$ has the smaller necksize-sum $4\rho_A \leq 4R(\alpha)/\pi = 4[1-\sqrt{1/2}]/[2-\sqrt{1/2}] \approx .906$.
(ii) There is an automorphism of the moduli space for rhombic pentagons induced

by the map $(l,t,b,r,s-b;\alpha) \mapsto (t,l,s-b,r,b;\pi/2-\alpha)$. The assumption that the surfaces are in the same connected component of the moduli space and have closed periods leads to a contradiction since the maximal necksize-sum is not symmetric under $\alpha \mapsto \pi/2-\alpha$. It may well be that the surfaces are not in the same connected component; note that, unlike the isosceles case, we believe that the rhombic surface with k bubbles on the central arc are in different connected components for different k.

References

[A] A.D. Alexandrov: Uniqueness theorems for surfaces in the large, Vestnik Leningrad University, **19(13)**: 5-8 (1958).

[Be] J. Berglund: PhD-thesis, University of Massachusetts, Amherst, in preparation

[G] K. Große-Brauckmann: New surfaces of constant mean curvature, Math. Zeit. **214**, 527-565 (1993)

[GP] K. Große-Brauckmann, K. Polthier: Constant Mean Curvature Surfaces derived from Delaunay's and Wente's surfaces, SFB 288 preprint, TU-Berlin (1996), and to appear.

[Ka] H. Karcher: The triply periodic minimal surfaces of A. Schoen and their constant mean curvature companions. man. math. **64**, 291-357 (1989)

[Kp] N. Kapouleas: Complete constant mean curvature surfaces in Euclidean three-space. Ann. of Math. **131**, 239-330 (1990)

[KK] N. Korevaar, R. Kusner: The global structure of constant mean curvature surfaces. Invent. Math. **114**, 311-332 (1993).

[KKS] N. Korevaar, R. Kusner, B. Solomon: The structure of complete embedded surfaces with constant mean curvature, J. Diff. Geom. **30**, 465-503 (1989).

[K1] R. Kusner: Bubbles, conservation laws, and balanced diagrams. In: P. Concus, R. Finn, D. Hoffman, editors: Geometric analysis and domputer graphics. Springer New York 1991.

[K2] R. Kusner: Natural Lagrangian and Symplectic Structures for the Moduli Spaces of Constant Mean Curvature Surfaces and Related Geometric Variational Problems, preprint.

[KMP] R. Kusner, R. Mazzeo, D. Pollack. The moduli space of complete embedded constant mean curvature surfaces. Geom. Funct. Anal. (to appear).

[L] H.B. Lawson: Complete minimal surfaces in $\mathbb{S}^3$. Ann. of Math. **92**, 335-374 (1970)

[M] W.H. Meeks: The topology and geometry of embedded surfaces of constant mean curvature, J. Diff. Geom. **27**, 539-552 (1988)

Universität Bonn, Mathematisches Institut, Beringstr. 1, 53115 Bonn, Germany

E-mail address: kgb@rhein.iam.uni-bonn.de

Mathematics Department, University of Massachusetts, Amherst MA 01003, USA

E-mail address: kusner@gang.umass.edu